LEP Physics - An Overview

J. Mnich
CERN-EP,
CH 1211 Genève 23
E-mail: Joachim.Mnich@cern.ch

This article summarises recent results obtained by the four experiments ALEPH, DELPHI, L3 and OPAL at the LEP e^+e^- collider. The experimental results discussed here comprise a summary of the measurements of electroweak observables at the Z resonance, the measurement of W-pair production from the threshold up to $\sqrt{s} = 183$ GeV and results from the searches for Higgs bosons and Supersymmetric particles at these highest energies attained in e^+e^- collisions. The majority of the data discussed here is preliminary and reflects the status at the time of the conference.

1 Introduction

The Large Electron-Positron Collider (LEP) at CERN in Geneva started in 1989 to operate at centre-of-mass (cms) energies close to the mass of the Z. This first phase (LEP I) has been concluded in 1995. The four experiments collected a total of about 16 million decays of the Z into hadrons and leptons. This large data sample allows the very precise measurement of Z parameters and the test of the Standard Model [1] (SM) beyond the tree level. Many other physics results have been obtained, and are still obtained, from careful analyses of these data. Examples are tests of Quantum Chromodynamics, physics of the b-quark and the tau lepton and also searches for new particles.

In the autumn of 1995 the LEP machine began to raise in steps the centre-of-mass energy beyond the Z resonance. This has been possible after installation of additional superconducting radio frequency cavities required by the higher energy loss due to synchrotron radiation at higher beam energies. In preparation of the second phase (LEP II), marked by running at energies above the W pair production cross section, LEP was operated at cms energies between 130 and 140 GeV in November 1995. The W-pair production threshold, 161 GeV was reached in 1996 and the cms energy could be further increased to 172 GeV. In the following year, a high luminosity run was performed at a mean energy of $\sqrt{s} = 183$ GeV. Tab. 1 summarises the cms energies and the approximate luminosities collected by each experiment.

At LEP II the experiments have performed measurements of the $e^+e^- \rightarrow W^+W^-(\gamma)$ cross sections, the determination of the W mass and the study of triple gauge boson couplings. In addition, the increase in energy allowed the exploration of new kinematic regions in the search for new particles, in particular for the SM Higgs boson [2] and Supersymmetric (SUSY) particles. Other important fields investigated at LEP II are studies of fermion-pair production and two-photon physics.

In the following selected items on four of these topics are presented: Precision tests of the SM at the Z, W physics and the searches for Higgs bosons and SUSY particles at the highest energy.

2 Precision Tests of the SM

One of the major achievements of the first phase of the LEP experiments is the precise measurement of cross sections $e^+e^- \rightarrow \text{hadrons}(\gamma)$ and $e^+e^- \rightarrow \ell^+\ell^-(\gamma)$ around the Z resonance. From these measurements the properties of the Z can be derived with a precision which exceeds the expectations at the time the experiments began in 1989 [3].

Table 1: Summary of LEP operation: Listed are the approximate cms energies with the integrated luminosities collected by each of the four experiments.

$\sqrt{s}$ [GeV]	$\int \mathcal{L}\,\mathrm{d}t$ [pb^{-1}]
$\approx m_Z$	150
$130-140$	12
161	10
172	11
183	55

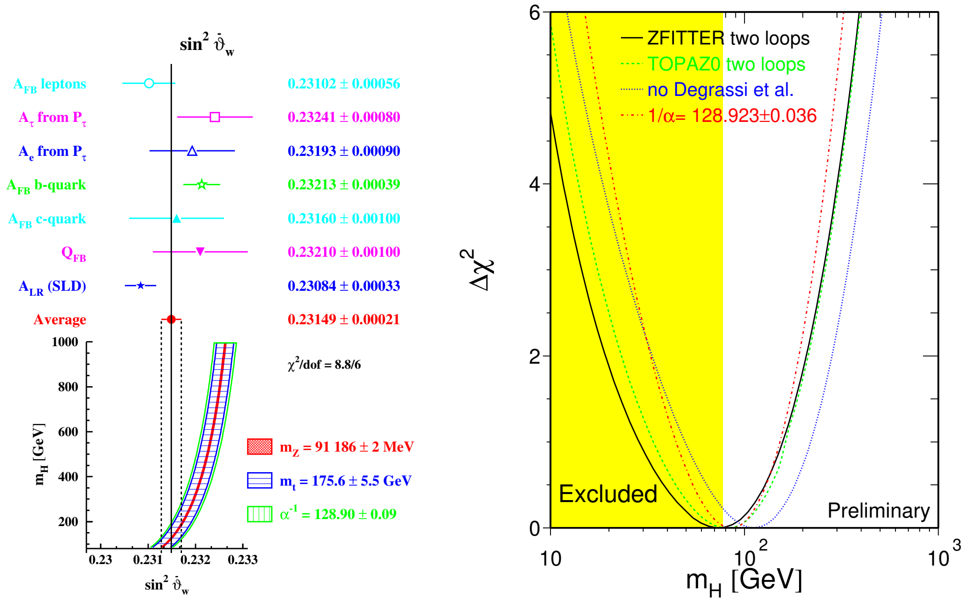

Figure 1: Left: Comparison of measurements of the effective weak mixing angle $\sin^2\bar{\vartheta}_W$ from different observables at LEP and by SLD. The measurements are compared to the SM expectation as a function of the Higgs mass. Right: Result of the SM fit for the Higgs mass using all experimental results on electroweak observables.

As an example the combined results for the mass, total width and the partial hadronic and leptonic width of the Z are [4]:

$$\begin{aligned} m_Z &= 91\,186.7 \pm 2.0 \text{ MeV} & \Gamma_Z &= 2\,494.8 \pm 2.5 \text{ MeV} \\ \Gamma_{\text{had}} &= 1\,743.2 \pm 2.3 \text{ MeV} & \Gamma_\ell &= 83.91 \pm 0.10 \text{ MeV}\,. \end{aligned} \tag{1}$$

From these numbers the partial decay width of the Z into invisible particles can be derived which in turn yields for the number of neutrino families $N_\nu = 2.993 \pm 0.011$.

Another important electroweak observable measured at LEP and by SLD is the partial decay width of the Z into b quarks, normalised to the total hadronic decay width, $R_\mathrm{b} = \Gamma_\mathrm{b}/\Gamma_{\text{had}}$. The current average $R_\mathrm{b} = 0.2173 \pm 0.0009$ agrees within less than two standard deviations with the SM expectation [5].

The measurements of forward-backward and left-right asymmetries and of tau-polarisation at the Z allow the precise determination of the effective weak mixing angle $\sin^2\bar{\vartheta}_W$. A comparison of $\sin^2\bar{\vartheta}_W$ measurements is shown in Fig. 1. Good agreement is observed between the results obtained from different observables and the average value is $\sin^2\bar{\vartheta}_W = 0.23149 \pm 0.00021$ with a $\chi^2 = 8.8$ for six degrees of freedom [5].

The measurements are compared to the SM calculation as a function of the Higgs mass using for the masses of the Z and the top quark and for the QED coupling constant α at m_Z the values indicated in the figure. The errors on these parameter lead to uncertainties in the calculation of $\sin^2\bar{\vartheta}_W$ which are indicated by the bands. The measurements are consistent

Table 2: The total cross section $e^+e^- \to W^+W^-(\gamma)$ at 183 GeV as measured by the LEP experiment with the combined value.

	σ_{WW}
ALEPH	15.51 ± 0.71 pb
DELPHI	16.01 ± 0.83 pb
L3	16.66 ± 0.73 pb
OPAL	15.52 ± 0.62 pb
combined	15.90 ± 0.41 pb

with Higgs masses between the lower bound given by the direct search for Higgs production at LEP (see below) and the upper theoretical limit of 1 TeV. The measured value of the weak mixing angle points to a low value for m_H.

The mass of the SM Higgs is determined more precisely in a fit to all electroweak measurements. In addition to the asymmetries, the measurements of the Z decay widths and the W mass are used. As the weak radiative corrections depend quadratically on the mass of the top quark its direct determination at the Tevatron is important to constraint m_H. This fit yields an estimate for the Higgs mass in the SM and a lower limit at 95% C.L. [5]:

$$m_H = 74^{+84}_{-45}\ \text{GeV} \qquad m_H < 250\ \text{GeV}\,. \tag{2}$$

The asymmetric errors reflect the logarithmic dependence of electroweak observables on the Higgs mass. Remaining theoretical uncertainties from higher order contributions are expected to be small. The χ^2 of this fit as function of the Higgs mass is shown in Fig. 1. Fits performed with the two programs ZFITTER [6] and TOPAZ0 [7] give very similar results when two-loop top corrections are implemented [8]. These corrections lead to a significant shift in the m_H value. Also shown in Fig. 1 is the χ^2 curve when a new calculation with reduced error of the QED coupling constant α at the mass of the Z is used [9]. A lower limit on m_H obtained previously from the direct search for the Higgs boson at LEP is shown as a band.

3 Physics of the W boson

Since the threshold for W-pair production was attained in 1996 the LEP experiments study the reaction $e^+e^- \to W^+W^-(\gamma)$. The main goals are the measurement of the cross section as a function of the energy, which together with the measurement of differential cross sections allows to study the couplings at the triple boson vertices, and the precise measurement of the W mass. Published results on W physics at LEP can be found in Ref. [10].

To date about 900 $e^+e^- \to W^+W^-(\gamma)$ events have been collected by each of the four collaborations, most of them at $\sqrt{s} = 183$ GeV. The preliminary cross sections measured at this energy by the four collaborations are shown in Tab. 2 together with the average value. This value is in very good agreement with the SM expectation as can be seen in Fig. 2. The average cross sections measured by the LEP experiments at three different cms energies follow the SM expectation and prove the existence of triple gauge boson couplings. Models with no ZWW vertex or only t-channel exchange of electron neutrinos are ruled out.

More information on the couplings of the W boson is contained in the differential distributions of the W production angle and the decay angles in the W rest frame. Limits on anomalous couplings of the W boson to the photon and the Z are derived from combined fits to the observed distributions and the total cross sections.

Assuming the W couplings to be real, obeying C-, P- and CP- invariance and setting the electric charge of the W to be equal to that of the electron, the most general ansatz for W couplings reduces to five parameters. These parameters and their SM model values are

$$\delta_Z = g_{ZWW} - \cot\Theta_W = 0 \qquad \kappa_\gamma = \kappa_Z = 1 \qquad \lambda_\gamma = \lambda_Z = 0\,, \tag{3}$$

where g_{ZWW} is the coupling at the ZWW vertex which is given by the weak mixing angle Θ_W. Some of these parameters are constraint by low energy measurements as well as by the

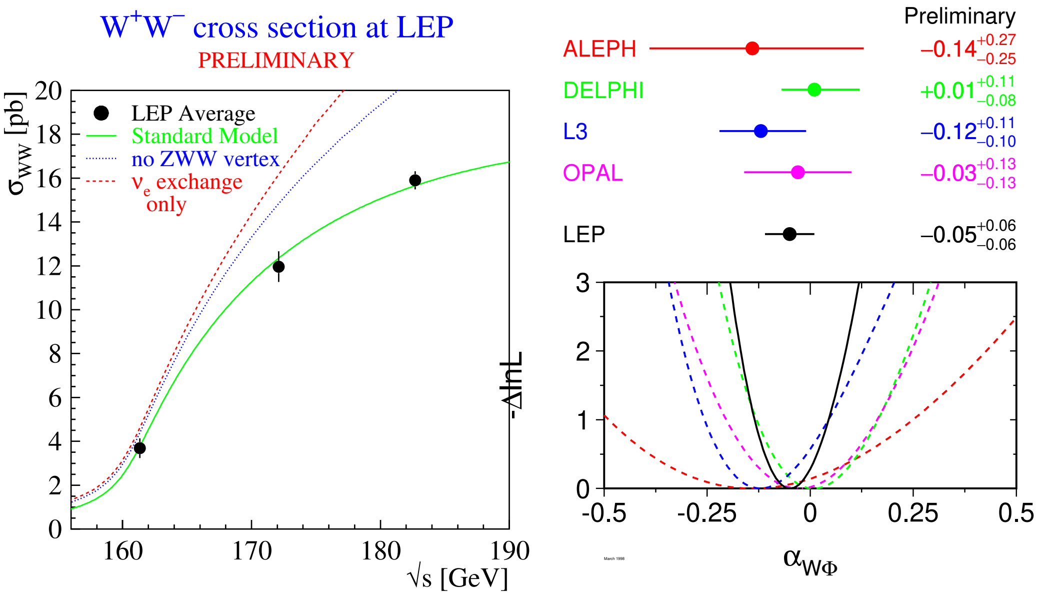

Figure 2: Left: Measurements of the cross section $e^+e^- \to W^+W^-(\gamma)$ at LEP. The combined measurements of the LEP experiments are compared to the SM and models without triple gauge boson couplings. Right: Study of anomalous triple gauge boson couplings at LEP. Results on the parameter $\alpha_{W\phi}$ are shown for the four experiments together with the combined value which is obtained from a superposition of likelihood curves.

precision data from LEP I. Therefore, anomalous couplings are defined by linear combinations which do not alter the gauge boson propagators at tree level [11]:

$$\alpha_{W\phi} = \Delta g_{ZWW} \cos^2\Theta_W \qquad \alpha_W = \lambda_\gamma \qquad \alpha_{B\phi} = \Delta\kappa_\gamma - g_{ZWW}\cos^2\Theta_W\,. \tag{4}$$

The deviation from the SM value is denoted as Δ.

The results of the studies performed at LEP so far show no indication for anomalous W boson couplings. As an example the results for $\alpha_{W\phi}$ are shown in Fig. 2. The LEP combined value is obtained from a superposition of the likelihood curves obtained by the four experiments.

An important measurement performed at LEP II is the precise determination of the mass of the W boson. A first value for m_W was derived from the total cross section measurement at the threshold, $\sqrt{s} = 161$ GeV, which is very sensitive to m_W. The combined LEP result is $m_W = 80.40^{+0.22}_{-0.21}$ GeV. At higher cms energies the W mass is obtained from direct reconstruction of the W decay products. To improve the resolution on the mass, a kinematic fit is performed using the precisely calibrated LEP beam energies. In addition, the masses of the two W bosons in an event are either constrained to be identical or the same within the width of the W.

Fig. 3 shows the reconstructed W mass distributions obtained by OPAL from the 183 GeV data for events with both W bosons decaying into hadrons and for events with one W boson decaying into leptons, as well as the combined distribution. The data are compared to the result of the fit for m_W, indicating the contributions from the signal and the remaining background, the latter being important only in the four-jet channel.

Combining the results obtained by the LEP experiments from the data taken at 161 GeV $\leq \sqrt{s} \leq 183$ GeV yields a value for the W mass of

$$m_W = 80.35 \pm 0.09 \text{ GeV}\,. \tag{5}$$

This number is in agreement with the measurement at $p\bar{p}$ colliders and both m_W determinations are of the same precision (see Fig 3). Also shown in this figure is the comparison

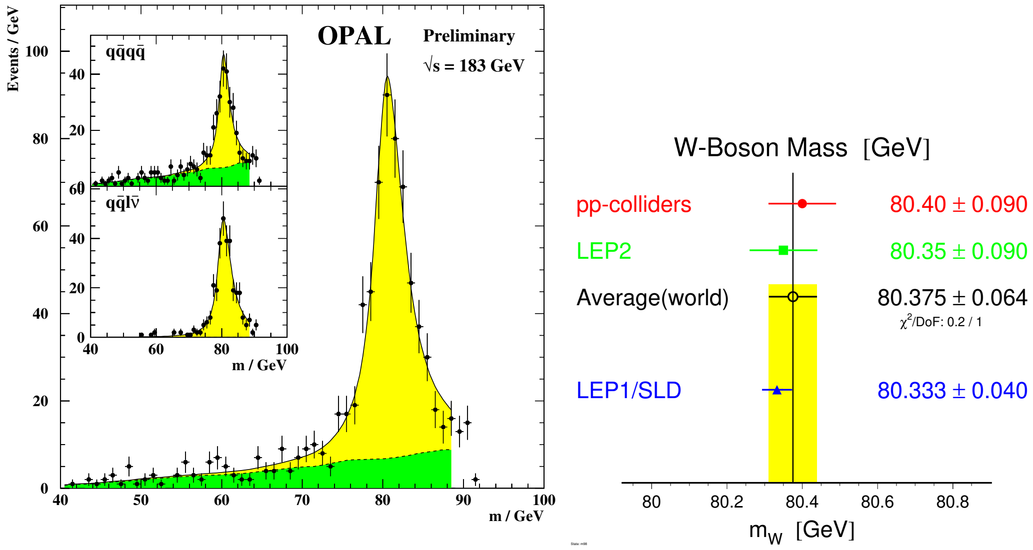

Figure 3: Left: Distribution of the reconstructed W mass obtained by OPAL from the 183 GeV data. Right: Comparison of direct W mass measurements from p$\bar{\rm p}$ colliders and LEP with the combined value. Also shown is the mass value derived from the measurements of electroweak observables at LEP I and SLD.

with the W mass derived from the measurements at the Z with even better precision. Here the W mass enters through the weak mixing angle $\cos\vartheta_{\rm W} = m_{\rm W}/m_{\rm Z}$ into cross sections and other observables. The excellent agreement of the direct measurement of $m_{\rm W}$ and the indirect determination at the Z can be considered an important success of the SM.

4 Search for Higgs Bosons

The production of SM Higgs bosons at LEP II would proceed mainly through the Higgs-strahlung diagram with small contributions from WW fusion. The range of Higgs masses which can be explored at a given cms energy is then limited by the fact that the Higgs boson is produced in conjunction with a real Z boson. Above this kinematic threshold the cross section $\rm e^+e^- \to ZH$ rises quickly to a sizeable level as compared to other SM processes. This results in a much better signal to background ratio as compared to Higgs searches performed at the Z resonance.

Following the decay modes of the Z and Higgs bosons four final states are distinguished in the search for the Higgs. In the mass range investigated the Higgs decays predominantly into b quarks ($\approx 84\%$), but also its decays into tau leptons and other quarks are considered: (i) $\rm HZ \to H\,q\bar{q}$ (four jets); (ii) $\rm \to H\,\nu\bar{\nu}$ (two acoplanar jets); (iii) $\rm \to H\,e^+e^-$, $\rm H\mu^+\mu^-$ (two jets and two leptons) and (iv) $\rm \to \tau^+\tau^-\,q\bar{q}$. The main backgrounds are fermion-pair production, in particular $\rm e^+e^- \to q\bar{q}(\gamma)$, four fermion final states $\rm e^+e^- \to W^+W^-$, ZZ and for $\rm H\,\nu\bar{\nu}$ the production of single W bosons $\rm e^+e^- \to We\nu$.

The most sensitive channel in the Higgs search is the four jet topology due to the high hadronic branching ratio of the Z. The tagging of b quarks is essential in all decay channels to suppress background. Kinematic fits are employed to improve the mass resolution on the hypothetical Higgs in candidate events. The fits exploit the fact that the two objects, jets or leptons, not associated to the Higgs should stem from a real Z boson.

No indication for Higgs boson production has been observed at LEP so far and only lower mass limits can be derived from the negative search results [12]. The hypothesis of Higgs boson production, with respect to the presence of background only, is then tested as a function of $m_{\rm H}$ taking into account candidate events and their significance for a given mass

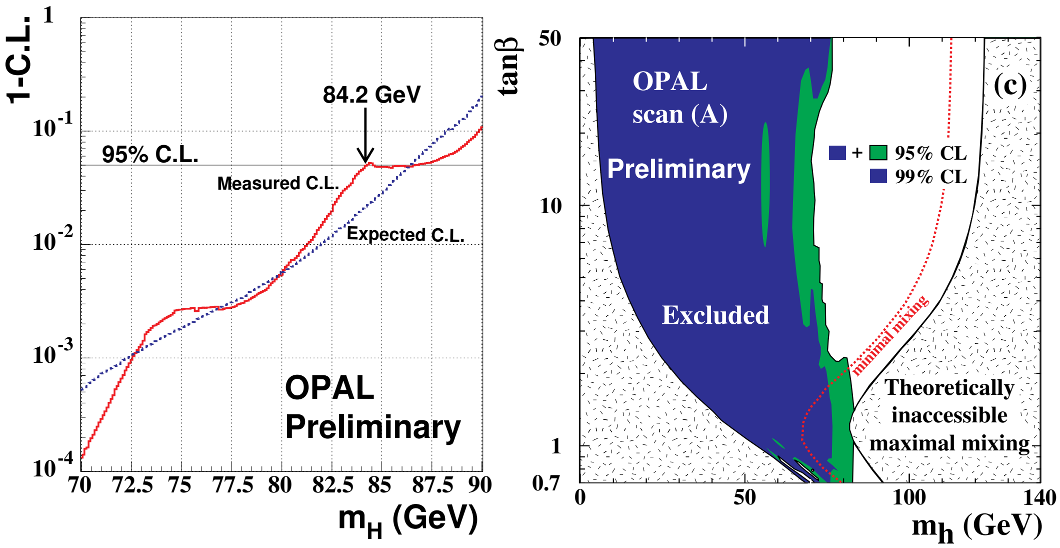

Figure 4: Left: Preliminary lower mass limit of the SM Higgs boson obtained by the OPAL experiment. Right: Lower mass limit on the h boson as a function of $\tan\beta$.

Table 3: Summary of preliminary limits on the SM Higgs boson H and the MSSM Higgs boson h obtained by the LEP experiments.

ALEPH	$m_{\rm H} > 88$ GeV	$m_{\rm h} > 73$ GeV
DELPHI	$m_{\rm H} > 84.4$ GeV	$m_{\rm h} > 74.4$ GeV
L3	$m_{\rm H} > 87.6$ GeV	
OPAL	$m_{\rm H} > 84.2$ GeV	$m_{\rm h} > 70.0$ GeV

value. Fig. 4 shows the confidence level (1-C.L.) for Higgs production as a function of $m_{\rm H}$ as obtained by OPAL from which the experimental mass limit is derived. In addition to the measured C.L. the expected C.L. is also shown. It is derived from a large number of Monte Carlo experiments simulating the data sample and detector performance in the background only hypothesis. The experimental lower limits (95% C.L.) on the SM Higgs boson mass obtained by the LEP experiments are summarised in Tab. 3.

In SUSY models the Higgs sector consists of more than one fundamental scalar particle. In the Minimal Supersymmetric (MSSM) extension of the SM five Higgs bosons are predicted $\rm H^+$, $\rm H^-$, H, h and A, where h is believed to be the lightest one. The LEP experiments have searched for the production of the two additional neutral bosons in the reactions $\rm e^+e^- \to hA$ and $\rm e^+e^- \to hZ$. The cross sections of these processes depend on the parameter $\tan\beta$, the ratio of the vacuum expectation values associated to the neutral Higgs bosons. The production of hA is dominant for large $\tan\beta$ values whereas the reaction $\rm e^+e^- \to hZ$, with an experimental signature very similar to the SM Higgs production discussed above, governs at low $\tan\beta$.

The combined result of the search for hZ and hA production as obtained by OPAL is presented in Fig. 4. No signal is observed and the lower mass limit for the h boson is shown as a function of $\tan\beta$. The limit obtained for small $\tan\beta$ is the same as for the SM Higgs boson and it reaches a minimum of 70 GeV at larger $\tan\beta$. Results of other LEP experiments are summarised in Tab. 3. Also shown in Fig. 4 are regions in the $\tan\beta$-$m_{\rm h}$ plane not allowed by the theory for two different mixing scenarios in the scalar quark sector and for the MSSM parameters assumed to be $m_0 = M_2 = 1$ TeV. Under these assumptions the LEP experiments start to exclude low values of $\tan\beta$.

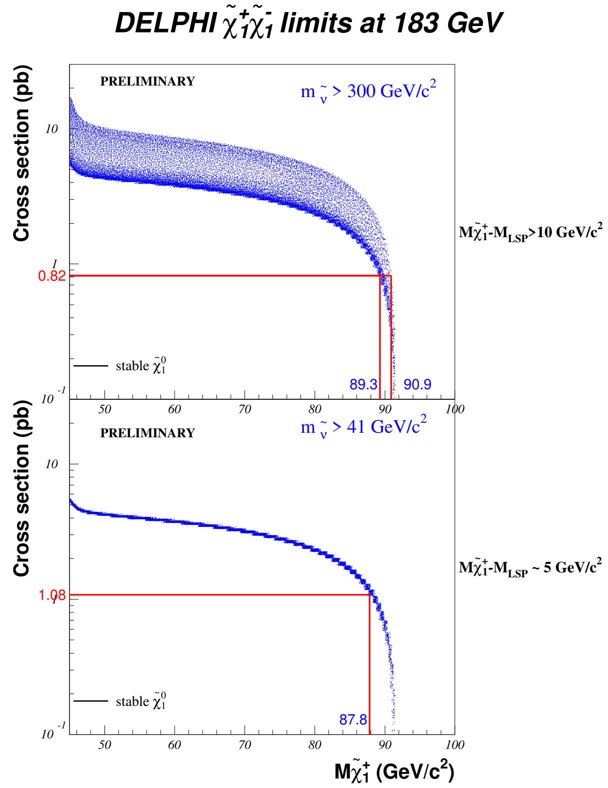

Figure 5: Expected cross section for chargino pair production at 183 GeV and the chargino mass limits obtained by DELPHI.

5 Search for SUSY Particles

The search for new particles predicted by SUSY [13] has been carried out by the LEP experiments from the Z resonance up to $\sqrt{s}$ = 183 GeV. Published results on searches for charginos, neutralinos and scalar leptons can be found in Ref. [14]. Three different type of models are investigated which can be distinguished by the type and nature of the lightest SUSY particle (LSP):

- gravity mediated SUSY breaking with a heavy gravitino $\tilde{G}$ and the LSP being the lightest neutralino $\tilde{\chi}_1^0$;
- gauge mediated SUSY breaking with the $\tilde{G}$ as LSP;
- R-parity violating SUSY in which the LSP is unstable.

So far no sign for SUSY has been observed. A few examples of search results on the first two scenarios are discussed here.

In the MSSM high cross sections of the order of several picobarn are expected for a wide range of parameter space in the kinematically accessible region at LEP II, in particular for chargino pair production $e^+e^- \to \tilde{\chi}_1^+\tilde{\chi}_1^-$. Expected cross sections at $\sqrt{s}$ = 183 GeV as a function of the chargino mass are shown in Fig. 5. The two bands shown, obtained from MSSM parameter variations, correspond to a high scalar neutrino mass $m_{\tilde{\nu}}$ and to the lowest mass compatible with the limit obtained at LEP I. The chargino is assumed to be 10 GeV or 5 GeV heavier than the invisible LSP which guarantees that the chargino production could be observed experimentally. The expected cross section depends on $m_{\tilde{\nu}}$ because the t-channel exchange of scalar neutrinos interferes destructively with the s-channel boson exchange and it reaches a minimum for $m_{\tilde{\nu}} \approx 100$ GeV. From the non-observation of a signal upper limits on the chargino production cross section are set and converted into lower mass limits which

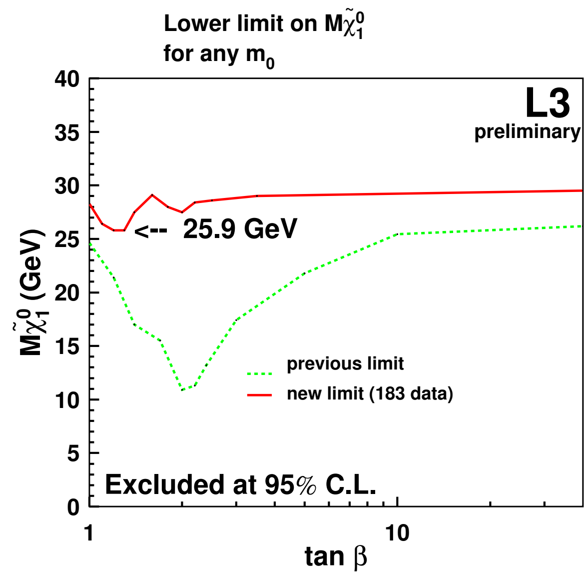

Figure 6: Preliminary lower mass limit on the lightest neutralino as function of $tan\beta$ obtained by the L3 experiment.

are in some cases close to the kinematic limit. Fig. 5 is from the DELPHI experiment and similar results are obtained by the other collaborations.

The negative results of the searches for chargino, neutralino and scalar lepton production can be combined and interpreted in the MSSM framework in terms of a lower mass limit of the lightest neutralino $\tilde{\chi}_1^0$. The result of such an analysis is shown in Fig. 6. The lower limit on $m_{\tilde{\chi}_1^0}$ obtained from scanning the MSSM parameter space is shown as a function of $\tan\beta$. Due to the dependence of the cross sections and decay signatures for charginos, neutralinos and scalar leptons on MSSM parameters the individual searches for these processes contribute in different regions to the neutralino mass limit. The limit obtained at 95% C.L. from the data at $\sqrt{s} = 183$ GeV is

$$m_{\tilde{\chi}_1^0} > 25.9 \text{ GeV} \tag{6}$$

which is valid for all values of the scalar mass parameter m_0 and for $\tan\beta > 1$. A limit of $m_{\tilde{\chi}_1^0} > 30$ GeV is achieved if a large value for m_0 is assumed.

Single photon events and multi-photon events with missing energy could provide evidence for SUSY [15]. Examples are the production of heavier neutralinos and their subsequent radiative decay $e^+e^- \rightarrow \tilde{\chi}_2^0\tilde{\chi}_1^0 \rightarrow \tilde{\chi}_1^0\tilde{\chi}_1^0\gamma$ or, in gauge mediated SUSY models, the radiative decay of neutralinos into gravitinos $e^+e^- \rightarrow \tilde{\chi}_1^0\tilde{\chi}_1^0 \rightarrow \tilde{G}\tilde{G}\gamma\gamma$. In the SM the reaction $e^+e^- \rightarrow \nu\bar{\nu}\gamma(\gamma)$ gives rise to observed final states with photons and missing energy.

Fig. 7 shows the energy spectrum of single photon events and the recoil mass distribution of di-photon events with missing energy as measured by L3 at $\sqrt{s} = 183$ GeV. In both cases good agreement with the SM expectation is observed, in the total rate as well as in the shape of the distributions.

The study of di-photon events can then be used to set upper limits on the cross section for the process $e^+e^- \rightarrow \tilde{\chi}_1^0\tilde{\chi}_1^0 \rightarrow \tilde{G}\tilde{G}\gamma\gamma$ and to interpret them in terms of mass limits for SUSY particles. The excluded mass of the lightest neutralino as a function of the scalar electron mass obtained by ALEPH is shown in Fig. 8. It is compared to the kinematically allowed region of the CDF event [16] which could be explained by production of scalar electrons [17]. A large portion of the allowed region is excluded at LEP proving unlikely this explanation of the CDF event.

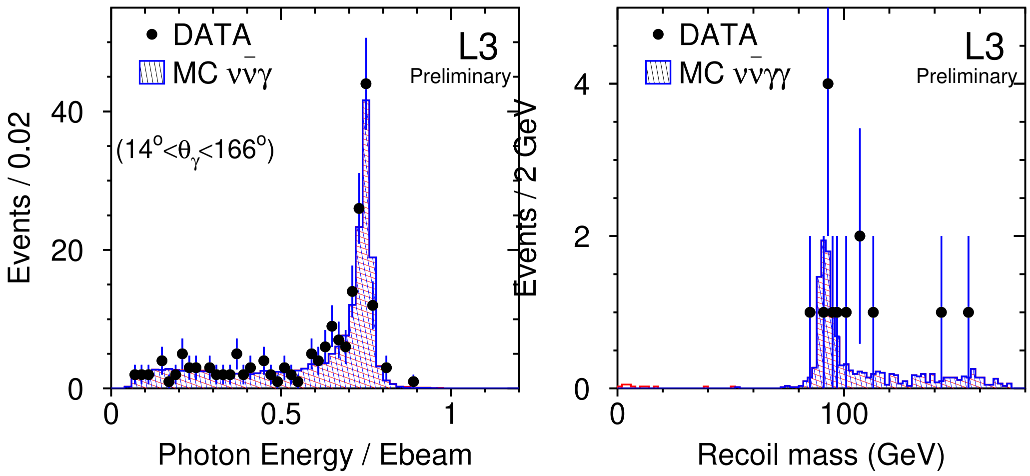

Figure 7: The single photon spectrum and the recoil mass distribution in di-photon events measured by L3 at $\sqrt{s} = 183$ GeV.

In SUSY models with a superlight gravitino also the process $e^+e^- \to \tilde{G}\tilde{G}$ can be relevant and, when accompanied by initial state radiation, modify the observed single photon spectrum. If the mass of the next-to-lightest SUSY particle exceeds the cms energy this is the only accessible reaction to produce SUSY particles [18]. The single photon spectrum observed by L3 at 183 GeV yields the exclusion for the gravitino mass shown in Fig. 8. From the data a lower mass limit at 95% C.L. of

$$m_{\tilde{G}} > 8.0 \cdot 10^{-6} \text{ eV} \tag{7}$$

is set which corresponds to a lower limit of the SUSY breaking scale of $\sqrt{F} > 181.9$ GeV.

6 Conclusion and Outlook

The LEP collider and the four experiments have been operated successfully at cms energies from the Z pole up to 183 GeV. Many precise measurements have been performed with the large amount of data collected, for example the determination of the properties of the Z and W bosons. The SM of electroweak and strong interactions is confirmed up to an energy of $\sqrt{s} = 183$ GeV. The search for new physics has been extended up to this energy. No sign of Higgs boson production or of SUSY has been observed by the experiments. The negative search results for new particles yield many improved lower mass limits.

The energy of the LEP collider will be further increased up to $\sqrt{s} \approx 200$ GeV with the goal of collecting in total 500 pb^{-1} per experiment above the W-pair production threshold. This will allow the more precise determination of W parameters and to extend the kinematic range in the search for new particles. For example the SM Higgs boson could be discovered up to a mass of $m_H \approx 100$ GeV.

7 Acknowledgements

I would like to thank my colleagues from the LEP experiments for providing preliminary results from the recent run, in particular A. Blondel, W. de Boer and P. Mättig. Also, I am grateful to S. Mele and M. von der Mey for the careful reading of the manuscript.

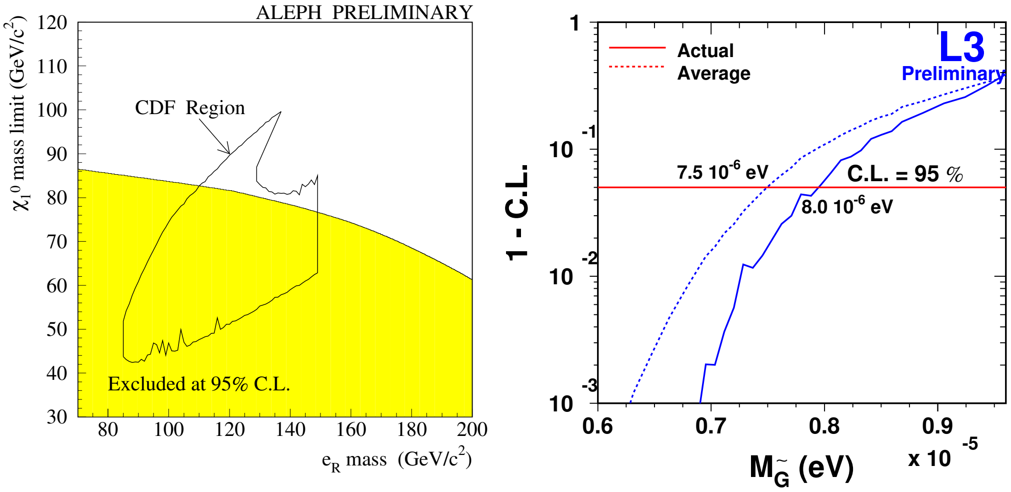

Figure 8: Left: Excluded region in the $m_{\tilde{\chi}_1^0} - m_{\tilde{e}}$ plane from ALPEH. Right: Mass limit on a superlight gravitino obtained by L3.

References

1. S.L. Glashow, *Nucl. Phys.* B **22**, 579 (1961); S. Weinberg, *Phys. Rev. Lett.* **19**, 1264 (1967); A. Salam, "Elementary Particle Theory", Ed. N. Svartholm, Stockholm, "Almquist and Wiksell" (1968), 367.
2. P.W. Higgs, *Phys. Lett.* B **12**, 132 (164); F. Englert and R. Brout, *Phys. Rev. Lett.* **13**, 321 (1964); G.S. Guralnik *et al*, *Phys. Rev. Lett.* **13**, 585 (1964).
3. "Z Physics at LEP I", CERN Report CERN 89-08 (1989), eds. G. Altarelli, R. Kleiss and C. Verzegnassi.
4. The LEP Coll. ALEPH, DELPHI, L3, OPAL, the LEP Electroweak Working Group and the SLD Heavy Flavour Group, Preprint CERN-PPE/97-154.
5. The LEP Electroweak Working Group, Internal Note LEPEWWG 98-01, (URL: http://www.cern.ch/LEPEWWG/stanmod/)
6. D. Bardin et. al., Preprint CERN-TH 6443/92, *Z. Phys.* C **44**, 493 (1989), *Nucl. Phys.* B **351**, 1 (1991), *Phys. Lett.* B **255**, 290 (1991).
7. G. Montagna *et al*, *Nucl. Phys.* B **401**, 3 (1993), *Comp. Phys. Comm.* **76**, 328 (1993).
8. G. Degrassi, P. Gambino and A. Sirlin, *Phys. Lett.* B **394**, 188 (1997).
9. M. Davier and A. Höcker, Preprint LAL 97-85.
10. ALEPH Coll., R. Barate *et al*, *Phys. Lett.* B **401**, 347 (1997), *Phys. Lett.* B **415**, 435 (1997), *Phys. Lett.* B **422**, 384 (1998), *Phys. Lett.* B **422**, 369 (1998); DELPHI Coll., P. Abreu *et al*, *Phys. Lett.* B **397**, 158 (1997), *E. Phys. J.* C **2**, 581 (1998), *Phys. Lett.* B **423**, 194 (1998); L3 Coll., M. Acciarri *et al*, *Phys. Lett.* B **398**, 223 (1997), *Phys. Lett.* B **407**, 419 (1997), *Phys. Lett.* B **413**, 176 (1997); OPAL Coll., K. Ackerstaff *et al*, *Phys. Lett.* B **389**, 416 (1996), *Phys. Lett.* B **397**, 147 (1997), *E. Phys. J.* C **1**, 395 (1998), *E. Phys. J.* C **2**, 597 (1998).
11. G. Gounaris, J.L. Kneur and D. Zeppenfeld in "Physics at LEP2", CERN Report 96-01, eds. G. Altarelli, T. Sjöstrand and F. Zwirner.
12. ALEPH Coll., R. Barate *et al*, *Phys. Lett.* B **412**, 155 (1997), *Phys. Lett.* B **412**, 173 (1997); DELPHI Coll., P. Abreu *et al*, *E. Phys. J.* C **2**, 1 (1998); L3 Coll., M. Acciarri *et al*, *Phys. Lett.* B **411**, 373 (1997); OPAL Coll., K. Ackerstaff *et al*, *Phys. Lett.* B **393**, 231 (997), *E. Phys. J.* C **1**, 425 (1998)), Preprint CERN-EP/98-029, subm. to *E. Phys. J.* C

13. P. Fayet, *Phys. Lett.* B **64**, 159 (1976), *Phys. Lett.* B **69**, 489 (1977); P. Fayet and S. Ferrara, *Phys. Rep.* C **32**, 249 (1977); H.P. Nilles, *Phys. Rep.* C **110**, 1 (1984); H. Haber and G. Kane, *Phys. Rep.* C **117**, 75 (1985).
14. ALEPH Coll., R. Barate *et al*, *E. Phys. J.* C **2**, 417 (1998), *Phys. Lett.* B **407**, 377 (1997); DELPHI Coll., P. Abreu *et al*, *E. Phys. J.* C **1**, 1 (1998); L3 Coll., M. Acciarri *et al*, *E. Phys. J.* C **4**, 207 (1998); OPAL Coll., K. Ackerstaff *et al*, *Phys. Lett.* B **389**, 616 (1996), *Phys. Lett.* B **396**, 301 (1997), *E. Phys. J.* C **2**, 213 (1998).
15. ALEPH Coll., R. Barate *et al*, *Phys. Lett.* B **420**, 127 (1998); DELPHI Coll., P. Abreu *et al*, *E. Phys. J.* C **1**, 1 (1998); L3 Coll., M. Acciarri *et al*, *Phys. Lett.* B **415**, 299 (1997), OPAL Coll., K. Ackerstaff *et al*, *Phys. Lett.* B **391**, 210 (1997), *E. Phys. J.* C **2**, 607 (1998).
16. CDF Collab., F. Abe *et al*, Preprint FERMILAB-PUB-98-024-E, subm. to *Phys. Rev. Lett.*
17. J.L. Lopez and D.V. Nanopoulos, *Phys. Rev.* D **55**, 4450 (1997).
18. A. Brignole, F. Feruglio and F. Zwirner, Preprint CERN-TH/97-339.